Predictive modeling of microbial biomineralization across scales

Atiyeh Ahmadi[1]* and Maria Dittrich[1,2]

1. Department of Physical and Environmental Sciences, University of Toronto Scarborough, 1265 Military Trail, Toronto, Ontario M1C 1A4, Canada

2. Department of Earth Sciences, University of Toronto, Toronto, Ontario, Canada

AUTHOR CONTACTS

Atiyeh Ahmadi (corresponding author): atiyeh.ahmadi@utoronto.ca

Maria Dittrich: m.dittrich@utoronto.ca

PREPRINT AND PEER-REVIEW STATUS

This manuscript is a non-peer-reviewed preprint submitted to EarthArXiv. It has not undergone formal peer review and has not been accepted for journal publication.

JOURNAL STATUS

The manuscript is being prepared for submission to *Communications Earth & Environment* (Nature Portfolio).

The full manuscript begins on the following page.

Predictive modeling of microbial biomineralization across scales

Atiyeh Ahmadi[1*] and Maria Dittrich[1,2]

[1*]Department of Physical and Environmental Sciences, University of Toronto Scarborough, 1265 Military Trail, Toronto, Ontario, M1C 1A4, Canada .

[2]Department of Earth Sciences, University of Toronto, Toronto, Ontario, Canada .

*Corresponding author(s). E-mail(s): atiyeh.ahmadi@utoronto.ca;
Contributing authors: m.dittrich@utoronto.ca;

Abstract

Microorganisms influence mineral formation and transformation in natural and engineered environments, with consequences for element cycling, contaminant mobility, and mineral records. Predicting these processes remains difficult because microbial activity, local aqueous chemistry, interfacial reactions, and mineral formation operate across different spatial and temporal scales. Here, we review molecular, geochemical, reaction–transport, biofilm- and cell-based, and data-driven models, focusing on what each can predict and how those predictions are tested experimentally. We explain the quantities that may connect models across scales, including ion binding, microbial activity, local chemical conditions, mineralization kinetics, and transport properties. Existing studies show stronger predictive development in geochemical and reactive-transport approaches than in connections between molecular interactions, microbial microenvironments, and mineral formation. We identify unresolved cross-scale relationships and discuss how spatially resolved measurements and independent experimental tests can strengthen predictive modeling of microbial biomineralization across scales.

Keywords: Microbial biomineralization; Predictive modeling; Molecular simulation; Reactive transport; Biofilm modeling; Multiscale modeling

1 Introduction

Microbial biomineralization refers to mineral formation in the presence of microorganisms, where microbial activity or interactions between microorganisms and their surrounding environment influence the process. Two broad modes are commonly distinguished: biologically controlled and biologically induced biomineralization. In biologically controlled biomineralization, mineral formation is regulated directly by cellular processes and specialized biological structures. In biologically induced biomineralization, microbial activity modifies the surrounding chemical environment and creates conditions that favor mineral precipitation [1, 2]. Such chemical changes can include shifts in pH, redox conditions, and the ionic composition of the surrounding aqueous solution. Cell surfaces and extracellular polymeric substances can also bind ions and provide reactive sites for mineral nucleation [1, 3]. Microbial biomineralization occurs in soils, sediments, aquifers, rocks, and engineered porous materials. Common products include carbonates, phosphates, silicates, oxides, and metal sulfides [2]. In natural systems, microbial activity contributes to carbonate formation in mats and microbialites and to phosphorus transformations associated with phosphate mineral formation in sediments [4–6]. The resulting minerals can influence element cycling and preservation of mineral records. In engineered systems, microbial precipitation is used for ground stabilization, carbon mineralization, and contaminant immobilization. Predicting these processes is relevant to both interpreting environmental mineral formation and designing mineral-based treatments.

Spatiotemporal prediction of microbial mineral formation remains difficult because biomineralization is controlled by coupled biological, chemical, and transport processes. Microbial metabolism can change local chemical conditions and mineral saturation. Mineral nucleation may also depend on cell surfaces, extracellular polymers, and pre-existing mineral phases. Transport governs the distribution of cells, dissolved reactants, and reaction products. Biofilm growth and pore structure can further modify local transport and reaction conditions [2]. These processes operate across spatial scales ranging from molecular interfaces to porous media and field systems. Their characteristic timescales also differ (Fig. 1). Therefore, models that resolve processes at one scale often simplify processes operating at other scales.

Computational approaches address different parts of this coupled process. Molecular simulations study ion association and interfacial interactions [3, 7], whereas geochemical models describe aqueous speciation, mineral saturation, and mineral reactions. Reaction–transport models couple microbial and chemical processes with transport and flow [8, 9]. Pore-scale, biofilm, and cell-based models represent spatial heterogeneity and microbial organization [10–12], while data-driven approaches relate measurements or simulation outputs to specified outcomes [13]. Predictive applications are particularly well developed for ureolytic microbially induced carbonate precipitation (MICP) in engineered porous media. Recent reviews have examined MICP and enzyme-induced carbonate precipitation (EICP) mechanisms, microfluidic observations, and upscaling for engineering applications [14]. We use these studies as the best-developed examples of coupled prediction, while including phosphate, other mineral systems, and natural environments where they clarify the limits of transfer between modeling approaches.

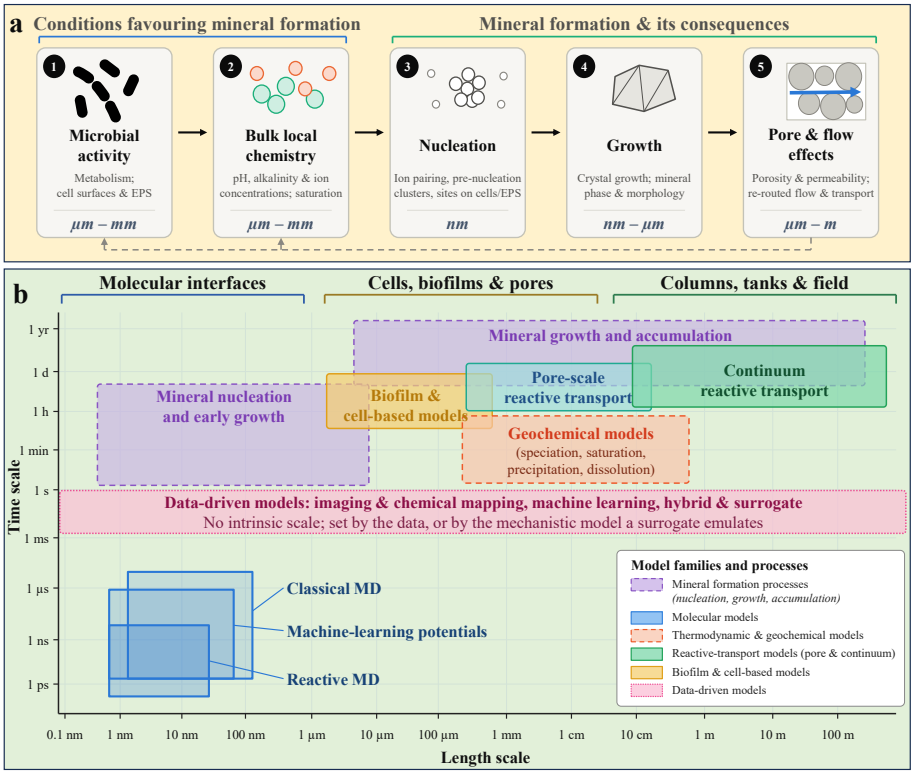


Fig. 1 Processes and modeling scales in microbial biomineralization. a, Microbial activity modifies local chemistry, which can promote nucleation, mineral growth, and subsequent changes in pore structure and flow. The brackets distinguish conditions favoring mineral formation from mineral formation and its consequences. **b**, Approximate spatial and temporal domains represented by major modeling approaches. Model domains overlap and are indicative. Data-driven methods have no intrinsic scale.

Prediction targets range from conditions favoring mineral formation to mineralization outcomes. How these predictions are evaluated is a separate question [15], discussed in Section 8.

Here, we review computational approaches used to study and predict microbial biomineralization across scales. For each approach, we ask which processes are represented, which quantities are predicted, and how those predictions are constrained and tested experimentally. We explain which quantities can connect molecular interactions, microbial microenvironments, biofilm organization, and mineral formation, distinguishing supported cross-scale relationships from those that remain proposed. We use this assessment to identify measurements and modeling strategies needed to improve prediction beyond the conditions in which individual models were developed.

2 What can models predict in microbial biomineralization?

Computational models represent biological, chemical, and physical processes through mathematical relationships, computational rules, or relationships learned from data. Under specified inputs and, where relevant, initial and boundary conditions, models calculate quantities that describe a system. These calculated quantities are predictions of the model, whether they describe equilibrium conditions, changes over time, or spatial distributions. How these predictions are constrained and evaluated is a separate question.

In microbial biomineralization, predicted quantities differ across spatial and temporal scales. Molecular simulations can estimate ion association, hydration, adsorption, and interfacial energetics [3, 7]. Thermodynamic and geochemical models calculate aqueous speciation and mineral saturation, and can estimate equilibrium mineral amounts or stable mineral phases under specified assumptions. Models incorporating reaction kinetics and transport can predict precipitation rates, mineral accumulation, spatial distributions, and changes in porous-media properties such as porosity and permeability [16–18]. Biofilm and cell-based models can represent microbial biomass, spatial organization, and local metabolic activity. When coupled to mineral reactions, these models can also predict spatial patterns of mineral formation [12]. Data-driven models estimate specified outcomes from experimental or simulation data, although these outcomes do not always correspond directly to mineral formation [13].

An important distinction is between predicting conditions that favor mineral formation and predicting whether, when, and where minerals actually form. For example, thermodynamic supersaturation indicates that precipitation is favorable, but does not establish whether a mineral will form within a given period. Similarly, ion binding and interfacial energetics do not by themselves determine mineral nucleation or growth rates. Predicting the timing, amount, mineral phase, and spatial distribution of mineral formation requires appropriate descriptions of mineral reactions and, depending on the system, transport, microbial biomass and associated metabolic reaction rates, and local chemical conditions [8, 9]. The quantities predicted by individual approaches provide different information about mineral formation and cannot always be directly transferred between modeling scales.

Model predictions can be evaluated using different approaches. Calibration, parameter identifiability, and evaluation against observations not used for parameter estimation address distinct questions about model interpretation and applicability [17, 19]. These issues are discussed in Section 8.

Table 1 summarizes the main processes represented, prediction targets, experimental constraints, and predictive limitations of the modeling approaches considered in this Review.

Representative mathematical and computational formulations, together with selected applications and their calculated quantities, are provided in Supplementary Table S1.

Table 1 Comparison of modeling approaches used in microbial biomineralization. For each approach, the table summarizes the main processes represented, predicted or inferred quantities, the main limitation for predictive interpretation, and representative studies.

Approach	Processes represented	Predicted or inferred quantities	Main limitation	Representative studies
Molecular models				
Classical MD	Ion, water, organic, & interfacial interactions	Ion coordination, hydration, adsorption	Force-field dependent; reactions not represented	[3, 20, 21]
Reactive MD	Bond rearrangement & proton transfer	Reaction pathways, early clusters	High cost; limited validated parameters for biological interfaces	[22, 23]
Free-energy	Rare molecular transitions	Free energies, barriers, pathways	Depends on collective variables	[24, 25]
Density functional theory	Electronic structure, small clusters, & mineral surfaces	Binding energies, reaction energetics, interfacial structure	High computational cost; limited system size	[26, 27]
ML potentials	Learned atomistic interactions	Ion pairing, nucleation pathways, structural transitions	Mostly mineral & solution systems	[28–30]
Thermodynamic & geochemical models				
Speciation & saturation	Aqueous equilibria & mineral stability	Species distributions, ion activities, saturation indices	Favorability does not establish precipitation	[31–33]
Precipitation / dissolution	Equilibrium or kinetic mineral reactions	Mineral amount & reaction rate	Spatial patterns require transport coupling	[10, 17, 34, 35]
Surface complexation	Protonation & ion binding	Surface charge & ion accumulation	Binding does not establish nucleation	[36–39]
Reaction–transport models				
Reaction–diffusion	Local reactions & diffusion	Mineral amount & spatial pattern	No explicit advection	[40–42]
Reactive transport	Reactions, chemistry, flow, & transport	Rates, mineral distribution, porosity, permeability	Sensitive to kinetics & parameter transfer	[16, 17, 43–45]
Pore-scale	Flow & reactions in pore geometry	Local mineralization, pore occlusion, hydraulic change	High cost; difficult upscaling	[10, 46–48]
Biofilm & cell-based models				
Continuum biofilm	Biomass growth, transport, & mineral reactions	Biomass & mineral distributions	Averages cellular heterogeneity; limited direct mineral applications	[49–51]
Individual- / agent-based	Cell behavior, EPS, & local interactions	Cell distributions & mineral clustering	Many biologically specific parameters	[12, 52]
Data-driven models				
Imaging / spectroscopy inference	Image & spectral relationships	Mineral abundance, morphology, distribution	Often inference rather than forecasting	[53–55]
ML prediction	Input–outcome relationships	Immobilization & material properties	Limited to target & training domain	[13, 56–58]
Hybrid / surrogate	Data-driven plus mechanistic models	Parameters & reduced simulation outputs	Surrogate uncertainty differs from model uncertainty	[59, 60]

3 Molecular models

In microbial biomineralization, molecular models are used to study ion association, hydration, adsorption, interfacial structure, and early nucleation processes near cell surfaces, extracellular polymers, and mineral interfaces.

3.1 Molecular dynamics

Classical molecular dynamics (MD) follows atomic motion using a predefined force field [61]. A force field defines the mathematical relationships used to calculate the potential energy and forces between atoms based on terms such as bonded interactions, electrostatics, and van der Waals interactions [62]. In microbial biomineralization, MD is commonly used to resolve the local structure and dynamics of aqueous ions, organic molecules, water, and mineral surfaces over nanometre length scales and typically nanosecond to microsecond time scales. The accuracy of calculated ion-pair structures, hydration environments, mineral–water interactions, and adsorption energies depends on the chosen force-field parameterization [62]. Calcium carbonate is a widely used model system for atomistic studies of biomineral nucleation and growth. Several $CaCO_3$ force fields have been developed and evaluated against properties such as calcite and aragonite crystal structures, Ca^{2+} and CO_3^{2-} hydration, ion-pairing energetics, and the relative stability of calcium carbonate phases [7, 62, 63]. Relative phase stability and factors affecting polymorph selection constitute an additional molecular-scale prediction target, although thermodynamic stability does not determine which mineral phase forms experimentally.

Recent MD studies have tested microbial carbonate and phosphate mineralization using experimentally defined biological systems. Gao et al. combined MD with laboratory experiments to study calcification of *Bacillus licheniformis*. Amino-acid components were used to approximate part of the extracellular polymeric substance (EPS) environment. The simulations resolved Ca–CO_3 association, multi-ion complexes, and precursor structures near the biological interface [3]. A study of MICP used MD to test how quartz surface chemistry and Ca^{2+} concentration affect $CaCO_3$ nucleation during siliceous-sand reinforcement. Surface hydroxyl density influenced the spatial distribution of $CaCO_3$, while higher Ca^{2+} concentrations promoted homogeneous nucleation and larger clusters [20]. Huang et al. used MD to study carbonic-anhydrase-mediated conversion of CO_2 to bicarbonate during carbonate biomineralization by *Paenibacillus mucilaginosus* [64]. MD was also combined with experiments on *Pseudomonas aeruginosa*-induced struvite formation to resolve pre-nucleation pathways under microbial influence [21]. Other MICP-related MD studies have focused more directly on mineral deposition. Wang and Yang modeled the deposition of calcite and aragonite units on $CaCO_3$ substrates and quantified the effects of temperature, impact velocity, and crystal structure on deposition behavior [65]. Although the model did not explicitly represent microbial cells or EPS, the study provides molecular-scale information on crystal deposition processes that occur during carbonate mineral formation.

3.2 Reactive molecular simulations

Classical force fields generally retain the bonding topology defined at the start of a simulation. This limits their use for processes that involve bond formation, bond breaking, or proton transfer. Reactive molecular dynamics removes this restriction by allowing bonding to change during the simulation. Reactive force fields such as ReaxFF use bond-order-dependent interactions to allow bond formation and breaking without explicitly calculating electronic structure at every time step [66].

Reactive MD has been used mainly to study early stages of mineral formation in aqueous and mineral systems. Wang et al. studied the effect of calcite and vaterite seeds on $CaCO_3$ ion-pair formation using ReaxFF. Calcite surfaces promoted attachment of ion pairs through proton-transfer processes more strongly than vaterite surfaces [22]. Reactive MD has also been used to study early formation of amorphous $CaCO_3$, where bond rearrangement and proton transfer contributed to the structure and kinetics of the developing mineral phase [67]. More recently, Chen et al. compared the effects of Na^+ and Mg^{2+} on $CaCO_3$ cluster nucleation and growth. Mg^{2+} formed stable Mg–carbonate associations and inhibited formation of ordered $CaCO_3$ structures more strongly than Na^+ [23].

Microbial activity can alter local pH, ion concentrations, and solution composition, creating chemical conditions in which such reactions occur. Reactive MD can resolve the resulting bond rearrangements and proton-transfer processes, while microbial metabolism is generally represented outside the atomistic model. Applications are constrained by computational cost and the need for validated reactive-force-field parameters, particularly for complex biomolecules and heterogeneous biological interfaces [63, 66].

3.3 Free-energy and enhanced-sampling methods

Some molecular processes involved in mineral formation are infrequently observed during conventional MD simulations. Ion association, dehydration, adsorption, and structural rearrangement can involve transitions that are rarely sampled in conventional MD. Enhanced-sampling methods such as umbrella sampling and metadynamics bias selected collective variables, including ion separation or coordination number, to estimate free-energy landscapes and barriers [68–70]. Results depend on the collective variables chosen and how biased sampling is corrected.

In biomineralization research, free-energy methods have been used mainly to study mineral nucleation and interfacial processes. Simulations characterized calcium carbonate prenucleation clusters as dynamic hydrated ionic assemblies [24]. More recent metadynamics calculations quantified the free energy of $CaCO_3$ ion-pair formation under external electric and magnetic fields [25]. ReaxFF metadynamics has also been used to resolve Ca^{2+} dissolution pathways and carbonate-associated surface passivation on tricalcium silicate [71]. Applications to explicitly modeled microbial surfaces and chemically realistic EPS remain limited relative to mineral–solution systems. Enhanced-sampling methods are most informative when the main question concerns a free-energy barrier, transition pathway, or metastable state that is difficult to sample with conventional MD.

3.4 Density functional theory

Density functional theory (DFT) provides quantum-mechanical estimates of electronic structure and energetics without requiring an empirical force field. DFT-based calculations have been used to study calcium carbonate ion association, hydration, mineral-surface interactions, and reaction energetics relevant to biomineralization [26, 27]. For example, DFT-based molecular dynamics has been used to study the early association of Ca^{2+} with carbonate and bicarbonate species in aqueous solution [26]. More recently, DFT calculations combined with microbial–mineral experiments were used to quantify Mg dehydration and organic–Mg binding energetics at calcite step edges during microbially influenced dolomitization [27]. DFT is generally restricted to smaller systems and shorter time scales than classical MD, but it can provide reference energetics for mechanistic interpretation and for training machine-learning interatomic potentials.

3.5 Machine-learning potentials

Machine-learning interatomic potentials extend quantum-mechanical descriptions to larger atomistic systems by learning energies and forces from reference electronic-structure calculations. They approximate the corresponding potential-energy surface at substantially lower computational cost [72].

Piaggi et al. developed an ab initio machine-learning potential for calcium carbonate that reproduced aqueous ion pairing, several solid $CaCO_3$ phases, and the calcite–water interface [28]. Wang et al. used a machine-learning interatomic potential to study calcium phosphate nucleation from prenucleation clusters to amorphous calcium phosphate [29]. The simulations resolved changes in cluster composition, hydration, proton exchange, and structural organization during nucleation. Deep-learning potentials have also been used to study the emergence of crystalline phases from amorphous precursors, showing how machine-learned atomistic models can access structural transitions that are difficult to follow with conventional quantum-mechanical simulations [30].

Machine-learning potentials expand the size and time scales accessible to atomistic modeling, but applications relevant to microbial biomineralization currently remain concentrated on mineral and solution phases. Explicit representation of chemically complex microbial surfaces and EPS remains an important area for further development.

4 Thermodynamic and geochemical models

Geochemical models commonly use thermodynamic relationships to calculate aqueous speciation, mineral saturation, and equilibrium partitioning among aqueous species, mineral phases, gases, and reactive surfaces. They can also represent time-dependent mineral precipitation and dissolution using kinetic rate laws [31].

4.1 Aqueous speciation and mineral saturation

Total dissolved concentrations alone do not determine mineral saturation; the activities of the dissolved species involved in the mineral-forming reaction are also required. Geochemical speciation models calculate the distribution of dissolved components among free ions and aqueous complexes while accounting for acid–base equilibria and non-ideal solution behavior [73, 74]. The calculated activities are used to determine the saturation state of a mineral. A positive saturation index indicates thermodynamic supersaturation, whereas a negative value indicates undersaturation.

Speciation and saturation calculations are particularly useful when microbial metabolism changes solution chemistry. Ureolysis and other alkalinity-generating processes can increase carbonate availability and favor $CaCO_3$ supersaturation [17]. Biological struvite formation provides an example involving a phosphate-bearing mineral. Leng and Soares observed that microbial growth increased solution pH, while dissolved orthophosphate and Mg^{2+} concentrations decreased during struvite precipitation. Mineral formation was associated with calculated supersaturation, showing how geochemical calculations can help interpret experimentally observed biomineralization [32].

Geochemical predictions also depend on the thermodynamic constants used to describe aqueous equilibria. Ion-association constants describe the equilibrium between free ions and dissolved complexes, while activity coefficients account for non-ideal solution behavior, including ionic-strength effects. McDonogh et al. showed that revising the Ca^{2+}–PO_4^{3-} association constant substantially changed the calculated distribution of aqueous calcium phosphate species. Their results identified $CaHPO_4^0$ as the dominant calcium phosphate ion pair near neutral pH [33].

Phosphate mineral formation in natural sediments presents a prediction problem. Studies of marine sediments have linked microbial phosphorus cycling to apatite accumulation and phosphorite formation [4, 5]. These observations provide evidence of microbial involvement in phosphorus mineralization, but do not by themselves predict the timing or spatial distribution of precipitation. Such predictions require information on local phosphate sources, aqueous chemistry, mineral reaction kinetics, and transport.

Saturation indices indicate the thermodynamic potential for mineral precipitation, but do not determine whether or when precipitation will take place. Supersaturated solutions may remain metastable when nucleation is kinetically limited. Microbial surfaces can promote heterogeneous nucleation, as suggested by observations of biological struvite formation [32]. Classical nucleation theory relates the energetic barrier to formation of a stable nucleus to competing bulk free-energy and interfacial-energy contributions [75]. However, mineral formation can also proceed through precursor-mediated pathways and particle attachment that are not fully described by classical nucleation theory [76, 77]. Applying nucleation models to microbial cell surfaces and chemically heterogeneous extracellular polymeric substances requires additional information on interfacial energetics and local chemical conditions.

4.2 Mineral precipitation and dissolution

Geochemical models can account for mineral precipitation and dissolution using equilibrium or kinetic formulations. Equilibrium formulations calculate the amounts of specified mineral phases based on mass balance and thermodynamic equilibrium with the aqueous solution. Kinetic formulations use rate laws to calculate changes in mineral amounts over time. The distinction becomes important when mineral reactions do not reach equilibrium over the timescale of changes in solution chemistry.

Both formulations have been applied to microbially induced carbonate precipitation. Nassar et al. represented calcite precipitation primarily using an equilibrium formulation and also evaluated a kinetic formulation [17]. Razbani et al. compared pore-scale MICP simulations with equilibrium and kinetic calculations for a well-mixed system implemented in PHREEQC [10]. Similar modeling considerations arise for phosphate minerals. Natividad-Marin et al. compared thermodynamic and kinetic approaches to struvite precipitation and showed that calculated saturation states and precipitated mineral mass depend on the available solution-composition information and thermodynamic assumptions. Predictions of nucleation and crystal growth rates additionally depend on kinetic parameters, including reaction-rate constants [34].

Experimental studies also show that microbial conditions can influence mineral precipitation kinetics. Paulo et al. found that phosphorus availability during growth altered the cell-surface properties of marine *Synechococcus*, which were associated with changes in subsequent calcium carbonate precipitation rates and mineral morphology [78]. Such observations provide experimental constraints on the biological and interfacial processes that may need to be represented in kinetic models. Experiments with *Synechococcus* further showed that calcite precipitation depends on solution composition and that nucleation at cyanobacterial surfaces can differ from expectations based on bulk supersaturation [79, 80].

Equilibrium and kinetic formulations describe different aspects of mineral reactions, but neither alone determines their spatial distribution. Predicting mineral accumulation along a column or within two- or three-dimensional domains requires coupling mineral reactions with transport and, where relevant, spatially varying microbial biomass and metabolic activity, as discussed in Section 5.

4.3 Surface complexation and ion binding

Microbial cell envelopes and extracellular polymeric substances contain reactive functional groups that can bind dissolved ions. Carboxyl, phosphoryl, hydroxyl, and amino groups contribute to surface charge and metal binding [37, 38, 81]. Surface complexation models describe these interactions using discrete surface sites and equilibrium constants for proton and metal binding [37, 39]. The protonation state of the surface sites changes with pH, which alters their affinity for dissolved cations. Competitive binding among ions can further change the fraction of available sites occupied by mineral-forming ions.

Surface complexation modeling has been applied most extensively to proton and metal adsorption on bacterial surfaces rather than directly to mineral nucleation [39]. Quantitative models have described proton binding and adsorption of divalent cations

such as Ca^{2+} and Mg^{2+} to bacterial cell-wall components [36, 38]. These interactions can influence biomineralization by concentrating mineral-forming ions at cell surfaces or within EPS. Experimental studies also show that negatively charged functional groups in EPS and cell envelopes can bind metal cations and create sites associated with extracellular mineral formation [81].

Surface complexation models can quantify ion binding and accumulation at microbial interfaces, but these quantities do not directly determine mineral nucleation rates. Connecting surface complexation with precipitation and growth models requires additional information on interfacial reactions and mineral formation kinetics, as discussed in Section 9.

5 Reaction–transport models

Reaction–transport models couple microbial growth and metabolism, chemical reactions, and mineral formation with transport. Formulations differ in the kinetic laws and representations of fluid motion, microbial distribution, and pore geometry.

5.1 Reaction–diffusion models

Reaction–diffusion models couple local reaction rates with the diffusion of dissolved species. In microbial biomineralization, reaction terms can represent microbial growth, substrate consumption, ion production, and mineral precipitation, while diffusion describes the redistribution of dissolved reactants and products. These models are most appropriate when local concentration gradients are important and advective transport is weak or absent.

Reaction–diffusion modeling has been applied mainly to carbonate biomineralization. Nishimura and Matsubara coupled bacterial growth with microbially induced carbonate precipitation and used a reaction–diffusion framework to reproduce spatial patterns of $CaCO_3$ formation in porous media [40]. A related model later incorporated ureolysis, microbial growth, chemotaxis, and electrostatic adsorption of microorganisms and dissolved ions. The simulated amount and spatial distribution of $CaCO_3$ were consistent with previously reported experimental patterns [41]. More recently, reaction–diffusion modeling was extended to photoautotrophic biomineralization on exposed rock surfaces. The model reproduced vertically localized microbial layers and progressive $CaCO_3$ accumulation observed in field samples [42].

Current reaction–diffusion applications remain concentrated on carbonate systems. The main limitation is the simplified treatment of fluid motion. Systems in which advection substantially redistributes microorganisms or dissolved reactants require a reactive-transport formulation.

5.2 Reactive transport models

Reactive transport models couple the transport of dissolved species and suspended microorganisms by advection, diffusion, and dispersion with microbial processes and geochemical reactions. In MICP, these processes can include microbial growth and decay, urea hydrolysis, aqueous speciation, and calcite precipitation and dissolution.

Microbial growth and metabolic rates may be formulated using Monod-type or other kinetic expressions, while attachment and detachment describe exchanges between suspended and attached biomass. Models can also account for changes in porosity and permeability as minerals accumulate. Reactive transport modeling of microbial biomineralization has been developed most extensively for MICP in porous media [8, 9, 16].

Ebigbo et al. developed a Darcy-scale model in 2012 that coupled ureolysis, aqueous chemistry, microbial biomass, calcite precipitation, and porous-media flow [8]. Hommel et al. subsequently revised the model using experimentally constrained ureolysis kinetics and evaluated its performance against additional column and radial-flow experiments [16]. Nassar et al. (2018) applied apparent ureolysis kinetics calibrated using separate column experiments to a meter-scale tank under transient, non-uniform flow. Tank hydraulic and transport parameters were calibrated using bromide-tracer observations, whereas the calcite measurements were not used to fit the predicted mineral accumulation [17]. The model assumed constant activity of attached microorganisms, an approximation whose applicability depends on the conditions studied. Field-scale models have also been used to examine how injection strategy, well spacing, bacterial distribution, and treatment chemistry influence the spatial distribution of $CaCO_3$ [9, 82].

Subsequent studies have investigated how model parameters and treatment conditions influence predicted mineral distributions. Faeli et al. calibrated a reactive transport model against six column experiments and examined the effects of microbial activity, attachment efficiency, and treatment protocol through parameter-sensitivity analysis [43]. Models of biostimulated MICP have incorporated experimentally calibrated apparent ureolysis kinetics and tested how kinetic parameters and treatment conditions influence the amount and spatial uniformity of calcite precipitation [44]. For shallow submerged MICP, Li et al. demonstrated that fluid-density-driven flow, bacterial detachment, and the representation of boundary conditions affect predicted $CaCO_3$ distributions [45]. Computationally efficient formulations have also been developed. A one-dimensional PHREEQC model calculates ureolysis, calcite precipitation, porosity change, and calcite supersaturation through space and time [83], while recent simulations have investigated longer-term porosity evolution during MICP [84].

The influence of model parameters and boundary conditions depends on the system under investigation. Parameter-sensitivity analyses have identified microbial activity and attachment as important controls under some treatment conditions [43], while comparisons of alternative flow and boundary-condition representations have shown their importance for submerged systems [45]. Continuum-scale formulations also average processes within the pore space, which can obscure localized concentration gradients and mineral accumulation; pore-scale models instead resolve these processes within explicitly described pore geometries.

5.3 Pore-scale models

Pore-scale models simulate fluid flow, solute transport, microbial processes, and mineral formation within the pore spaces of porous media. Pore geometries can be represented in two or three dimensions using idealized or image-based structures, or

approximated as networks of connected pores and throats. These approaches allow the spatial distribution of mineral formation to be related to pore structure, local flow paths, reactant transport, and, where included in the model, microbial distribution and metabolic activity.

Pore-scale MICP models have progressed from simplified pore networks to fully coupled simulations with increasingly realistic geometry and biological processes. Early pore-network models combined microbial growth, geochemical reactions, and transport to investigate scale dependence in MICP reaction rates [46]. Direct numerical and lattice-Boltzmann approaches later coupled pore-scale transport, geochemical reactions, and bacterial activity, allowing local gradients in pH, ureolysis, and calcite precipitation to be resolved [10]. Recent models additionally incorporate bacterial transport and attachment, calcite detachment, heterogeneous pore structure, and evolving mineral surfaces [11, 47]. Image-based simulations using X-ray computed tomography have linked three-dimensional changes in pore structure caused by MICP to local hydraulic behavior [48]. Phase-field approaches have also connected experimentally constrained precipitation kinetics with pore-scale $CaCO_3$ crystal growth and morphology [85].

The porousRTFoam micro-continuum framework developed by Li and Yang couples flow, reactive transport, biomass evolution, and mineral reactions while representing evolving pore structure [86].

Pore-scale resolution increases computational cost, and effective reaction and transport relationships need to be assessed before use at larger scales [10, 46]. Their transferability is discussed in Section 9.

6 Biofilm and cell-based models

Biofilm and cell-based models describe how microbial spatial organization influences local chemical conditions and mineral formation. Metabolic models provide a complementary description of microbial activity. Genome-scale metabolic models predict feasible metabolic fluxes under specified growth and nutrient conditions and can inform biological rates that enter biomineralization models. In MICP, genome-scale metabolic modeling has been combined with experiments to study how the carbon-to-nitrogen ratio affects intracellular urease activity and biomineralization by *Sporosarcina pasteurii* [87].

6.1 Continuum biofilm models

Continuum biofilm models describe biomass as a spatially varying concentration or volume fraction rather than as individual cells. Local rate equations describe microbial growth and substrate consumption, while dissolved species are transported through or around the biomass. Additional processes, such as biomass attachment, spreading, detachment, or extracellular polymer production, can also be incorporated depending on the model. This representation is appropriate when the research question focuses on biofilm-scale structure and the collective behavior of the microbial community.

Direct applications to microbial biomineralization remain limited. Zhang and Klapper modeled biofilm, water, and calcite as interacting continuous phases within a pore

and coupled biofilm activity to ureolysis, aqueous chemistry, and mineral precipitation [49]. More recently, Starnoni and Sanchez-Vila coupled biomass growth with flow and reactive transport to study microbially enhanced carbonate mineralization for carbon storage [50]. Their model linked biomass-mediated changes in local chemistry to calcite precipitation within the pore space. Recent micro-continuum biofilm models have also incorporated biomass growth, attachment, spreading, and flow-induced detachment, although without mineral formation explicitly included [51]. Such developments provide a more detailed representation of biofilm dynamics that can be coupled with mineral reactions.

The averaging inherent in continuum models limits their ability to capture cell-to-cell heterogeneity and discrete microbial interactions.

6.2 Individual-based and agent-based models

Individual-based and agent-based models treat microorganisms as discrete entities with their own position and state. Model rules can describe growth, division, movement, mechanical interactions, substrate uptake, enzyme production, and extracellular polymer secretion. Dissolved chemical species are commonly represented as continuous concentration fields that interact with the discrete cells. NUFEB provides a general framework for large three-dimensional individual-based simulations of microbial communities with coupled biological, chemical, and mechanical processes [52].

Direct applications of individual-based and agent-based models to microbial biomineralization remain sparse. Zhao et al. coupled bacterial growth, urease activity, extracellular polymer secretion, and discrete-element interactions with $CaCO_3$ formation [12]. Experimental measurements were used to constrain model parameters, and the simulations linked bacterial concentration, spatial distribution, urea concentration, and porous-medium geometry to $CaCO_3$ clustering and morphology. Monte Carlo analysis was also used to evaluate uncertainty associated with enzyme secretion, catalytic kinetics, and diffusion parameters [12]. The model shows how microbial spatial organization and local biological activity can be connected directly to mineral morphology.

The increased biological detail introduces additional parameters for cellular growth, mechanics, secretion, and spatial interactions. Independent measurement of these parameters can be difficult, which increases uncertainty in model parameterization.

6.3 Representing mineral formation in microbial models

Biofilm and cell-based models also differ in how mineral formation is modeled. Continuum approaches commonly describe precipitation as a local reaction rate or an evolving mineral volume fraction coupled to biomass and aqueous chemistry [49, 50]. Discrete-cell approaches can couple mineral formation more directly to cell position, local enzyme activity, EPS production, and mineral clustering [12].

The treatment of mineral formation determines which microbial processes can influence the simulated mineral pattern. Continuum formulations capture feedbacks

among biomass growth, solution chemistry, mineral accumulation, and pore occlusion. Explicit cell-based formulations can additionally capture spatial variation among microorganisms and their locally produced enzymes or extracellular polymers. The cell-based biomineralization models reviewed here do not yet combine detailed microbial organization with molecular-scale ion binding, nucleation, and subsequent crystal growth. Connecting these processes across scales remains an important direction for predictive microbial biomineralization models.

7 Data-driven models

In microbial biomineralization, data-driven models use imaging, spectroscopy, experimental measurements, or simulation outputs to identify relationships associated with mineral amount, mineral phase, spatial distribution, or resulting physical properties of the mineralized material.

7.1 Models using imaging and spectroscopy

Optical imaging and chemical imaging (spectroscopy) can quantify mineral abundance, morphology, composition, and spatial relationships between minerals and microbial structures. Data-driven analysis can extract quantitative information from measurements that are difficult to interpret manually. Common approaches include image segmentation, feature extraction, dimensionality reduction, and classification.

Recent MICP studies have used data-driven imaging methods to quantify mineral precipitation and pore structure. Zi et al. combined synchrotron micro-computed tomography with a genetic-algorithm-enhanced multilevel segmentation method to separate precipitated $CaCO_3$, sand grains, and pores [53]. The resulting three-dimensional maps quantified pore structure and the spatial distribution of mineral precipitation. More recently, automated image segmentation was applied to microfluidic pore networks containing *Sporosarcina pasteurii* to quantify $CaCO_3$ coverage, particle density, and feature size across large image datasets [54]. The analysis showed that pore geometry influenced the size and spatial distribution of mineral deposits.

Spectroscopic measurements provide complementary information on mineral chemistry and structure. In broader biomineralization research, interpretable machine learning has been applied to Raman spectra to distinguish biotic from abiotic apatite using band positions, widths, and intensities [55]. The analysis associated classification with carbonate substitution and structural disorder, providing chemically interpretable spectral features rather than only a classification label. Data-driven analysis of Raman or hyperspectral measurements during microbial biomineralization remains relatively limited. Confocal Raman microscopy can provide two- or three-dimensional chemical maps at micrometer-scale spatial resolution, although volumetric measurements can require long acquisition times. These measurements can provide information on mineral identity and spatial chemical heterogeneity for comparison with spatially resolved models of microbial mineral formation.

7.2 Machine-learning models

Machine-learning models learn statistical relationships between measured inputs and a specified outcome. In microbial biomineralization, the prediction target can range from mineral or contaminant immobilization to physical properties of mineralized materials.

Prediction of mineralization-related outcomes remains relatively uncommon. Qiang et al. trained a deep neural network to predict uranium immobilization by *Bacillus subtilis* from pH, temperature, uranium concentration, bacterial concentration, and reaction time [13]. More recently, ensemble learning combined with Bayesian optimization and SHAP analysis was used to predict Pb immobilization during MICP and identify combinations of pH and treatment conditions associated with stable carbonate formation [56]. In contrast, machine learning in MICP has been used more extensively to predict downstream engineering properties. Gradient-boosting models have predicted the unconfined compressive strength of MICP-treated sands from soil properties, treatment conditions, bacterial measurements, and calcite content [57]. Explainable-AI models have further used feature-importance and SHAP analyses to identify variables associated with predicted strength [58].

Calcite content is already used as an input in models that predict the mechanical strength of MICP-treated materials [57, 58]. Such models predict the mechanical response of mineralized materials rather than $CaCO_3$ formation itself. Data-driven models can target mineral amount, mineral phase, or two- and three-dimensional mineral distributions, depending on the available measurements and modeling objective. Other models predict biomineralization-associated immobilization outcomes [13, 56].

7.3 Hybrid and surrogate models

Hybrid and surrogate models provide ways to combine data-driven methods with mechanistic models of microbial biomineralization. Hybrid models use learned relationships together with process-based simulations. These relationships can be used to estimate parameters that are difficult to measure directly. Surrogate models replace repeated evaluations of computationally expensive simulations with faster approximations, making parameter estimation, sensitivity analysis, and uncertainty analysis more practical.

One recent MICP application combined convolutional and recurrent neural networks, an attention mechanism, and XGBoost to estimate interparticle parameters for discrete-element simulations of MICP-treated calcareous sand [59]. The predicted parameters were subsequently used in discrete-element simulations and compared with experimental stress–strain behavior. Surrogate modeling has also been applied to reactive-transport simulations of MICP. Scheurer et al. developed surrogate models to approximate a computationally expensive reactive-transport model of MICP. They used measured calcite volume fractions at eight positions along a sand column to estimate probability distributions for four model parameters, while accounting for uncertainty introduced by the surrogate models [60].

Physics-informed neural networks (PINNs) provide another way to combine data-driven learning with mechanistic constraints. PINNs incorporate governing equations and boundary conditions into the training objective [88]. Recent reactive-transport

applications have embedded advection, dispersion, and nonlinear reaction kinetics within neural-network surrogates [89]. Their use could allow spatial or temporal biomineralization measurements to be combined with known reaction and transport equations when experimental data are limited.

8 Connecting models with experiments

Experimental measurements can be used to estimate model parameters, study parameter identifiability, or evaluate model predictions. Calibration estimates model parameters using experimental observations, whereas validation evaluates agreement between model outputs and observations. Comparisons with measurements not used for calibration provide an additional assessment of model performance. Distinguishing among these roles is important when interpreting agreement between models and experiments.

8.1 Parameter estimation

Parameters in microbial biomineralization models describe microbial growth, metabolic activity per cell or per unit biomass, reaction kinetics, ion binding, diffusion and transport, microbial attachment, and mineral precipitation. Some parameters can be determined from independent experimental measurements, whereas others are estimated by fitting model outputs to observations. However, different parameter combinations may reproduce similar observations, making it difficult to identify individual parameter values. Parameter estimation requires consideration of parameter identifiability and uncertainty.

Hommel et al. combined independently measured whole-cell ureolysis kinetics with inverse modeling of column and radial-flow experiments to estimate biofilm-density and attachment parameters [16].

Parameter identifiability depends on the measurements available. Bulk pH, ion concentrations, biomass, or total mineral content constrain system-level changes but may not show where minerals form or distinguish competing reactions. Spatially and temporally resolved measurements add information about mineral distribution, microbial organization, and local chemistry, yet different mechanisms can still produce similar spatial patterns. Combining measurements can reduce ambiguity without necessarily identifying unique parameter values.

8.2 Calibration and validation

MICP reactive-transport studies differ in how model parameters are constrained and predictions are evaluated. Nassar et al. evaluated the transfer of apparent ureolysis kinetics calibrated using separate columns to a meter-scale tank with transient, non-uniform flow. Tank flow and transport were constrained using bromide-tracer observations, while the predicted calcite accumulation was compared with tank measurements not used for fitting the calcite prediction [17]. More recently, Wang et al. estimated apparent ureolysis parameters under different biostimulation treatments

and compared predicted average $CaCO_3$ content over successive treatment cycles with measurements from treated sand columns [44].

Model evaluation also depends on whether experimental measurements correspond to the predicted quantities. Predictions of mineral amount require quantitative measurements of mineral formation, whereas predictions of spatial mineral distribution require spatially resolved measurements. Predictions of mineral identity require mineralogical or spectroscopic characterization. When mineral formation is attributed to microbial activity, abiotic controls under comparable chemical and transport conditions can help assess the biological contribution. Differences in local pH and mineral saturation must also be considered before attributing precipitation to direct interactions with microbial surfaces or extracellular polymeric substances.

In data-driven models, measurements collected at different locations or time points within the same experiment may be correlated. Evaluating models using independent experimental replicates, such as columns or biofilms not included in training, helps assess performance without sharing correlated measurements between training and testing. Evaluation under different chemical conditions, treatment protocols, or spatial scales additionally provides information on model transferability.

8.3 Uncertainty and model transferability

Uncertainty in model predictions refers to the range of plausible predicted outcomes arising from incomplete knowledge of model parameters, experimental conditions, and the processes represented. In microbial biomineralization, uncertainty can arise from measurement errors, estimated microbial and mineral reaction rates, initial and boundary conditions, and simplifications in how biological, chemical, and transport processes are described. Sensitivity analysis tests how changes in selected parameters or model inputs affect predicted mineral amounts and distributions. In MICP models, such analyses have identified ureolysis kinetics, microbial attachment and detachment, and treatment conditions as important controls on model outputs [16, 43, 45]. PHREEQC-based modeling has also examined the sensitivity of calcite precipitation to biomass and reaction parameters under specified treatment conditions [83]. Bayesian inference provides a complementary approach by combining experimental observations with prior information to estimate parameter distributions and propagate parameter uncertainty to model predictions. Scheurer et al. further demonstrated that accounting for uncertainty introduced by surrogate models can reduce overconfidence in inferred parameters and predicted calcite distributions [60].

The applicability of estimated parameters can depend on the conditions under which they were determined. For example, metabolic rates measured for suspended cells may differ from those of attached biomass, while effective attachment and reaction parameters can depend on solution chemistry and flow conditions. Hommel et al. reported that an earlier MICP model no longer adequately reproduced experimental observations after changes in solution chemistry. They revised the ureolysis formulation using whole-cell measurements and recalibrated the model with additional experimental data [16]. In studies of biocement dissolution, Ribeiro and Gomez used dissolution kinetics calibrated from batch experiments to predict mineral dissolution

Table 2 Forms of evidence used to evaluate model predictions in microbial biomineralization. The table distinguishes evaluation designs according to the observations and conditions used to assess model outputs. These categories are not ranked or mutually exclusive. The conclusions supported by each comparison depend on the prediction target, calibration procedure, and experimental design. References provide illustrative examples (not necessarily independent demonstrations of each evaluation category).

Evaluation approach	What is evaluated	What it does not establish on its own
Calibration fit	Agreement with observations used to estimate model parameters, including inverse modeling of MICP experiments [16]	Parameter identifiability, performance on independent observations, or transferability
Held-out observations within an experiment	Agreement with observations withheld from model calibration, such as measurements from selected times or locations [16]	Performance on an independent experimental unit; measurements within the same experiment may remain correlated
Independent experiment under similar conditions	Agreement with measurements from a separate experimental run, column, or biofilm that was not used for model calibration [16]	Applicability under different microbial, chemical, or transport conditions
Cross-condition evaluation	Agreement under changed chemistry, microbial populations, or flow conditions, with parameter adjustments explicitly reported [16, 44]	Applicability at another spatial scale or to a different mineral system
Cross-scale evaluation	Agreement at a different spatial scale using specified transferred model relationships or parameters, such as column-calibrated kinetics evaluated in a meter-scale tank [17]	Applicability to other mineral systems or validity of all unresolved biological and pore-scale processes
Field-scale comparison	Agreement with in situ measurements under documented calibration and boundary conditions, including reactive-transport modeling of field MICP observations [90]	Parameter transfer without site-specific calibration or performance beyond the tested field conditions

in soil columns, but found that some parameters may require site-specific calibration [35]. These studies show that a model formulation may remain applicable while the parameters needed to describe a particular system require further experimental constraints.

8.4 Evidence for predictive claims across conditions and scales

Model evaluation studies agreement with calibration observations, performance on independent experimental units, or applicability under different chemical, biological, transport, or spatial-scale conditions. These comparisons address different questions and should be interpreted in relation to the predicted quantities, parameters adjusted, and measurements used for evaluation. The corresponding evaluation approaches and their limitations are summarized in Table 2.

Cross-scale evaluation requires specifying which model quantities or relationships were transferred, whether their assumptions remain appropriate, and which parameters were estimated again. Agreement at one scale does not establish performance at another. These considerations motivate the relationships discussed in Section 9.

9 Combining models across scales

Microbial biomineralization involves processes operating across molecular, cellular, biofilm, pore, and larger spatial scales. Models developed at these scales calculate different quantities, and combining them does not require representing every process within a single simulation. Instead, the prediction target determines which processes need to be represented explicitly and which can be described using information obtained at another scale. The main challenge is identifying the relationships that connect these quantities and determining whether they remain applicable across spatial and temporal scales (Fig. 2).

9.1 Quantities transferred between models

Molecular models can estimate ion association, binding free energies, and interfacial interactions that may inform the thermodynamic description of ion binding at microbial surfaces. Translating these quantities into equilibrium parameters requires consistent definitions of the chemical species, surface sites, and thermodynamic conditions. However, a molecular binding affinity does not directly determine a nucleation or precipitation rate. Connecting molecular interactions to mineral formation requires additional relationships describing nucleation and growth kinetics [3, 38].

Connections between microbial and transport models involve different quantities. Cell-based and biofilm models can describe microbial abundance, spatial organization, and metabolic activity. Local reaction rates can be calculated from microbial biomass and biomass-specific metabolic rates, provided that their dependence on local chemical conditions is represented. These rates can then enter reaction–diffusion or reactive-transport models to calculate changes in aqueous chemistry and mineral accumulation. The relationship is not necessarily fixed, because metabolic activity can vary with nutrient availability, pH, and the physiological state of the microorganisms.

Pore-scale models provide another connection by relating local transport, microbial distribution, and mineral accumulation to effective reaction and hydraulic properties [10, 46]. These quantities can inform continuum-scale models without explicitly resolving individual pores. However, averaging local concentrations and reaction rates does not necessarily preserve their relationships, particularly when reactions are nonlinear or microorganisms and minerals are distributed heterogeneously. Effective parameters may also change as mineral accumulation modifies pore geometry and flow. Transferring pore-scale information requires relationships that account for the conditions and spatial scale over which the quantities are averaged.

9.2 Limits of cross-scale relationships

Cross-scale connections are limited not only by spatial resolution but also by differences in the assumptions used to represent biological and mineral reactions. Model outputs describing related processes are not necessarily interchangeable.

The importance of a particular connection also depends on the prediction target. Predicting total mineral accumulation may require fewer details about local microbial organization than predicting the location or onset of precipitation. Similarly, reproducing an average reaction rate does not necessarily establish that a model can

predict local mineral distributions. Mineral formation can also introduce feedbacks: precipitation changes the available reactive surfaces and, in porous media, may alter transport and flow. These changes can influence subsequent microbial activity and mineral reactions. Models that do not represent such feedbacks may be sufficient for some prediction targets but not for others.

Differences in temporal scales introduce further limitations. Ion association and changes in aqueous speciation may occur much faster than microbial growth, biofilm development, or mineral accumulation. Mineral formation may also be delayed under supersaturated conditions because of nucleation kinetics. Relationships derived under equilibrium or steady-state assumptions need to be reconsidered when predicting time-dependent mineral formation. The appropriate level of detail depends on which processes influence the predicted quantity over the timescale of interest.

Evidence for these cross-scale connections differs. Reactive-transport models have coupled microbial kinetics, aqueous chemistry, and transport using experimentally constrained parameters [8, 16]. Nassar et al. further evaluated column-calibrated ureolysis kinetics in a meter-scale tank, with flow and transport constrained by tracer observations and without fitting the predicted calcite accumulation to tank mineral measurements [17]. In contrast, Qin et al. investigated the scale dependence of effective reaction rates numerically, without independently evaluating the resulting relationships at a larger experimental scale [46]. Quantitative connections between molecular interactions at heterogeneous microbial interfaces, biofilm-scale mineral nucleation, and larger-scale mineral accumulation remain less established. These examples distinguish experimentally evaluated transfer, computational investigations of scale dependence, and cross-scale relationships that still require quantitative development.

9.3 Developing and evaluating cross-scale predictions

A useful approach is to begin with a defined mineralization outcome and identify the relationships required to calculate it. For example, predicting the onset and spatial distribution of $CaCO_3$ formation in a photosynthetic biofilm requires connecting microbial activity to local chemical conditions, local chemistry to mineral saturation, and mineral saturation to precipitation kinetics. Biofilm and reaction–diffusion models could describe the effects of microbial activity and transport on local pH and dissolved inorganic carbon. Geochemical calculations could then estimate mineral saturation, while kinetic formulations would be needed to predict mineral formation through time. Molecular or surface-complexation models could provide additional information on ion binding at microbial interfaces where those interactions are relevant to the prediction.

These connections would need to be constrained and evaluated using measurements corresponding to the quantities calculated. Local chemical measurements could help evaluate the predicted microenvironment, while imaging and spectroscopy could provide information on microbial organization, mineral identity, and spatial mineral accumulation. Measurements collected over time could establish when mineral formation becomes detectable, although detection does not necessarily coincide with nucleation.

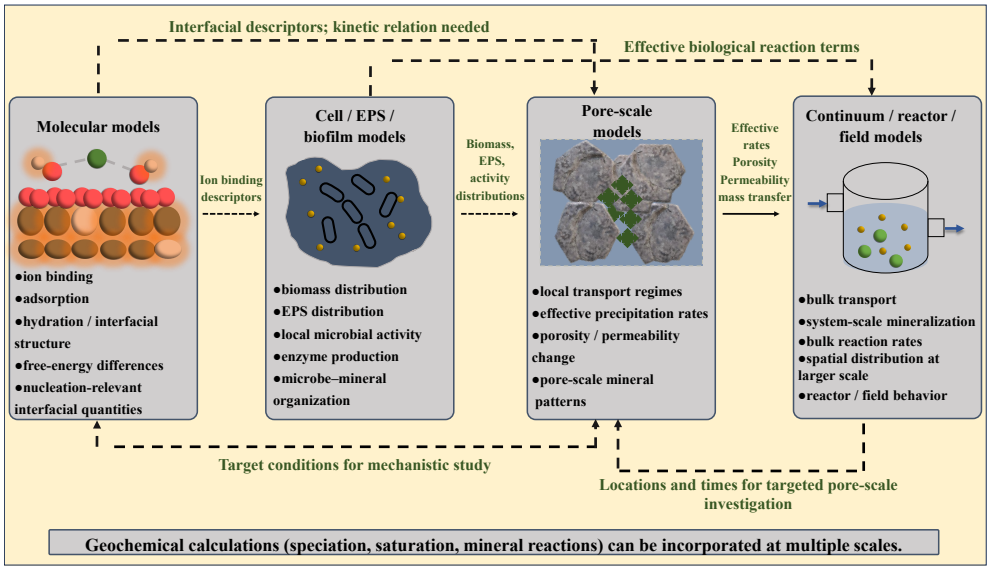


Fig. 2 Cross-scale information flow in predictive microbial biomineralization models. Molecular models provide information on ion association, binding, and interfacial energetics. Cell- and biofilm-scale models describe microbial distributions, EPS, and metabolic activity, while pore-scale models represent local transport, mineral formation, and changes in pore structure. Continuum and field-scale models describe larger-scale transport and mineral accumulation. Arrows indicate the transfer of quantities or relationships between modeling approaches. Solid arrows indicate examples of couplings implemented in the reviewed literature, whereas dashed arrows indicate illustrative or less-developed links; neither line style alone establishes independent experimental validation.

Model development can also proceed from larger to smaller scales. Differences between predicted and observed mineral distributions may indicate that local transport, microbial heterogeneity, or mineral reaction kinetics are not adequately represented. More detailed molecular or cell-based models can then be used to investigate candidate processes, followed by experiments designed to determine whether the additional relationships improve predictions at the original scale. Data-driven methods may also help estimate relationships that are difficult to derive mechanistically, although their applicability depends on the conditions represented in the training data.

The same approach can be applied to other mineral systems, but the relationships and parameters cannot necessarily be transferred unchanged. Models of carbonate precipitation driven by ureolysis, for example, do not directly describe phosphate mineralization in sediments, where microbial transformations, aqueous equilibria, mineral reactions, and transport conditions differ.

10 Conclusions and outlook

The value of a model of microbial biomineralization depends not only on the processes it represents, but also on the quantities it is intended to predict. The modeling approaches reviewed here calculate different quantities, including ion association, aqueous speciation, mineral saturation, microbial reaction rates, mineral amount, phase, spatial distribution, and resulting material properties. These quantities answer different questions.

The interpretation of model predictions also depends on how they are constrained and evaluated experimentally. Agreement with observations used for calibration does not necessarily establish parameter identifiability or applicability under different conditions. Bulk measurements may also be insufficient to distinguish among processes or spatial patterns. For example, similar total mineral amounts may result from different distributions of microbial activity, reaction rates, and transport. Combining bulk chemistry with spatially and temporally resolved measurements of microbial organization, local chemical conditions, and mineral formation can provide additional information, although different mechanisms may still produce similar observations.

Models representing alternative mechanisms can identify experimental conditions under which their predictions differ. Experiments designed around those differences can then test which processes matter for the specified mineralization outcome. Data-driven approaches may help estimate difficult relationships, provided their uncertainty and applicability are assessed using appropriate measurements.

Connecting models across scales provides an additional opportunity. Molecular interactions, microbial activity, and pore-scale transport can inform larger-scale predictions when quantitative relationships between their outputs are established. However, the quantities transferred between models do not necessarily retain the same interpretation or applicability across biological, chemical, and spatial conditions. Some physicochemical parameters can be applied across different systems under appropriate thermodynamic conditions, whereas biological and effective reaction parameters may depend on microbial physiology, local chemistry, and transport. Developing cross-scale models requires identifying which relationships can be transferred, which parameters need to be constrained for a particular system, and how the resulting predictions can be evaluated experimentally.

The next challenge in predictive microbial biomineralization modeling is to establish the relationships that connect molecular interactions, microbial activity, local chemistry, transport, and mineral formation, and to determine when these relationships support predictions beyond the conditions under which they were developed. Such an approach can move the field from separate descriptions of biomineralization processes toward experimentally supported predictions of when, where, and how minerals form across scales.

11 Appendix

Table S1: **Representative mathematical and computational formulations used in microbial biomineralization modeling.** The equations show general model families and are not necessarily reproduced from the cited studies. Selected studies indicate examples of application, not identical mathematical implementations.

Approach	Representative formulation and calculated quantities	Selected studies and interpretation
Molecular models		
Classical MD	$m_i\ddot{\mathbf{r}}_i = -\nabla_i U_{\mathrm{FF}}(\mathbf{R})$. Atomic trajectories evolve under a prescribed, generally fixed-topology force field. *Calculated quantities:* Ion coordination, hydration, adsorption, interfacial structure.	Gao et al. use MD with organic components representing aspects of microbial interfaces to examine calcium–carbonate association and early structures [3]. This formulation does not generally represent bond formation or proton transfer.
Reactive MD	$m_i\ddot{\mathbf{r}}_i = -\nabla_i U_{\mathrm{react}}(\mathbf{R})$. In ReaxFF-type models the reactive potential depends on coordination-dependent bond-order terms. *Calculated quantities:* Bond rearrangements, proton transfer, cluster structure and evolution.	Wang et al. investigate seed-dependent calcium carbonate ion pairing; Chen et al. assess Na^+ and Mg^{2+} effects on clusters [22, 23]. These are mineral/solution systems, not fully resolved microbial interfaces.
Free-energy / enhanced sampling	$F(q) = -k_{\mathrm{B}}T \ln P(q) + C$, where $P(q)$ is the *unbiased or reweighted* distribution of a collective variable. Umbrella sampling and metadynamics improve sampling of infrequent configurations. *Calculated quantities:* Free-energy profiles, metastable states and barriers associated with specified transitions.	Yuan et al. calculate calcium–carbonate ion-pair free energies using MD and metadynamics [25]; the inferred profile depends on the chosen collective variables and reweighting.
Density functional theory	$E_0 = \min_{n:\,\int n\,\mathrm{d}\mathbf{r}=N_e} E_{\mathrm{DFT}}[n]$. Electronic densities and energies are determined for specified atomic configurations, often using Kohn–Sham calculations. *Calculated quantities:* Binding and reaction energetics, electronic structure, mineral-surface interactions.	Di Tommaso and de Leeuw study early calcium carbonate association; Gao et al. combine mineral-interface experiments with DFT for microbial-organic effects on calcite surfaces [26, 27].

Continued on next landscape page

Supplementary Table S1 (continued)

Approach	**Representative formulation and calculated quantities**	**Selected studies and interpretation**
ML interatomic potentials	$E_\theta(\mathbf{R}, \mathbf{Z}) \approx E_{\text{ref}}$, with $\mathbf{F}_i = -\nabla_i E_\theta$. A learned potential approximates reference atomic energies and forces; simulations sample the learned energy landscape. *Calculated quantities:* Ion-pair free energies, local coordination, precursor structures, phase-related structural changes.	Piaggi et al. develop a DFT-trained calcium carbonate potential; Wang et al. simulate calcium phosphate cluster evolution [28, 29]. These mainly concern mineral–solution systems, not explicit microbial EPS.

Continued on next landscape page

Supplementary Table S1 (continued)

Approach	Representative formulation and calculated quantities	Selected studies and interpretation
Thermodynamic and geochemical models		
Aqueous speciation / saturation	$K_j = \prod_i a_i^{\nu_{ij}}$ at equilibrium; $\mathrm{SI} = \log_{10}(\mathrm{IAP}/K_{\mathrm{sp}})$. Activities, mass balances and equilibrium constants determine species distributions and saturation states. *Calculated quantities:* Aqueous activities and complexes; mineral saturation indices and equilibrium phase assemblages.	PHREEQC implements speciation and equilibrium calculations [31]; McDonogh et al. show how revised calcium–phosphate association constants alter calculated speciation [33]. A positive SI is not a precipitation-rate prediction.
Precipitation / dissolution	$\mathrm{d}M_s/\mathrm{d}t = R_{\mathrm{prec}} - R_{\mathrm{diss}}$. If a kinetic law is selected, R_{prec} may be written $kAf(\Omega)$; in equilibrium formulations mineral amount is determined by mass balance and thermodynamic constraints instead. *Calculated quantities:* Mineral mass (equilibrium or time-dependent); precipitation or dissolution rates when kinetics are represented.	Nassar et al. couple calibrated ureolysis kinetics to an *equilibrium* calcite treatment [17]. Natividad-Marin et al. compare equilibrium and kinetic struvite formulations [34]. The illustrative kinetic law is not Nassar's calcite equation.
Surface complexation	$\equiv S^- + \mathrm{Ca}^{2+} \rightleftharpoons \equiv SCa^+$, with equilibrium constants and site balances. Surface protonation and binding depend on pH, activities and site density. *Calculated quantities:* Surface occupancy and charge; adsorbed or surface-associated ion amounts.	Borrok et al. describe bacterial-surface proton binding; Thomas and Rice measure/model Ca^{2+} and Mg^{2+} binding to bacterial cell walls [36, 38]. Surface binding alone does not establish a mineral nucleation rate.
Reaction–transport models		

Continued on next landscape page

Supplementary Table S1 (continued)

Approach	**Representative formulation and calculated quantities**	**Selected studies and interpretation**
Reaction–diffusion	$\partial_t c_i = \nabla\cdot(D_i\nabla c_i) + R_i(\mathbf{c}, B, M)$. Chemical and biological reaction terms are coupled to diffusion, with no advective flux in this schematic form. *Calculated quantities:* Spatial and temporal concentrations, biomass, mineral amount or pattern.	Nishimura and Matsubara couple bacterial growth and carbonate precipitation in reaction–diffusion formulations [40]. The reaction function and mineral treatment are study-specific.
Continuum reactive transport	$\partial_t(\phi c_i) + \nabla\cdot(\mathbf{q}c_i - \phi\mathbf{D}_i\nabla c_i) = R_i$. R_i represents net sources/sinks per bulk volume in this simplified dissolved-species balance; other storage terms may be needed. *Calculated quantities:* Solute concentrations, reaction rates and mineral accumulation across columns or field domains.	Nassar et al. use PHT3D and independently calibrated apparent ureolysis kinetics to model a meter-scale experiment [17]; Minto et al. model field-scale MICP [9]. Reactive transport may be implemented at several spatial resolutions.
Pore-scale models	Fluid flow may be resolved in an explicit pore geometry, e.g. $-\nabla p + \mu\nabla^2\mathbf{u} = 0$, $\nabla\cdot\mathbf{u} = 0$ for creeping incompressible flow, coupled to advection–diffusion–reaction and evolving solids; pore networks and lattice-Boltzmann methods are alternatives. *Calculated quantities:* Local reactant fields and mineral deposits; pore blockage and hydraulic response.	Razbani et al. simulate direct pore-scale MICP [10]; Feng et al. couple lattice-Boltzmann flow, finite-element transport and cellular-automaton components [47]. Pore-scale is a spatial representation, not an alternative to reactive transport.

Continued on next landscape page

Supplementary Table S1 (continued)

Approach	Representative formulation and calculated quantities	Selected studies and interpretation
Biofilm and cell-based models		
Continuum biofilm	Illustrative biomass balance: $\partial_t B = \nabla\cdot(D_B \nabla B) + [\mu(\mathbf{c}) - k_d]B$. Biomass, solutes and mineral fractions can be represented as continuous fields or interacting mixture phases. *Calculated quantities:* Biomass and solute distributions; mineral volume fractions where precipitation is coupled.	Zhang and Klapper use a multiphase mixture framework with biofilm, mineral and water in a pore [49]. Their actual mixture equations should not be replaced by the illustrative biomass equation shown here.
Individual- / agent-based	Discrete microbes have positions $\mathbf{r}_i$, states and growth rules, e.g. $\dot{B}_i = \mu_i(\mathbf{c}(\mathbf{r}_i))B_i$. Mechanics and extracellular concentration fields couple agents to their environment. *Calculated quantities:* Cell distributions and activities; local mineral clusters when precipitation is explicitly coupled.	Zhao et al. integrate agent-based and discrete-element descriptions with carbonate mineralization [12]. NUFEB provides a general microbial individual-based platform, but the cited NUFEB study is not itself a mineral-precipitation demonstration [52].
Data-driven models		
Imaging / spectroscopy inference	$\widehat{\mathcal{M}} = g_\theta(I)$ for image segmentation; $\hat{y} = h_\theta(\mathbf{s})$ for a spectrum-derived label or property. Descriptors are measured or inferred from images/spectra. *Calculated quantities:* Mineral masks, abundance, morphology or class; inferred spectral mineral properties.	Zi et al. use genetic-algorithm-enhanced threshold segmentation of micro-CT scans [53]; Filanoski et al. use deep-learning segmentation of microfluidic mineral deposits [54]; Li et al. classify biotic/abiotic apatite Raman spectra [55]. These analyze existing samples rather than forecast new mineral formation.

Continued on next landscape page

Supplementary Table S1 (continued)

Approach	**Representative formulation and calculated quantities**	**Selected studies and interpretation**
ML outcome prediction	$\widehat{y} = f_\theta(\mathbf{x})$, fitted on input–outcome pairs with explicit definition of target y, training domain and evaluation split. *Calculated quantities:* Specified outcomes, such as adsorption/immobilization or mechanical strength.	Qiang et al. model uranium sorption/immobilization-related outcomes [13]; Talamkhani predicts strength of MICP-treated sand [57]. Neither should be described as directly forecasting mineral nucleation or spatial $CaCO_3$ deposition.
Hybrid / surrogate modeling	$\widehat{g}_\theta(\mathbf{p}) \approx g_{\mathrm{mech}}(\mathbf{p})$, where a fitted surrogate approximates a mechanistic simulator; hybrid schemes combine learned relations with process-based components. Approximation uncertainty may enter inference. *Calculated quantities:* Simulator outputs, inferred parameters, faster sensitivities or uncertainty estimates.	Scheurer et al. develop uncertainty-aware surrogate-based inference for computationally expensive reactive-transport applications [60]. Fu et al. combine ML-predicted interparticle parameters with discrete-element modeling of treated sand [59]; these targets are distinct from mineral-formation forecasting.

Acknowledgements. This manuscript is dedicated to the memory of Saeed Ghaziyani, a brilliant mind and a kind soul, whose joyful spirit, kindness toward others, and poetic way of seeing life and finding beauty in the world will always be remembered.

Declarations

Author contributions: A.A. and M.D. contributed to the conception of the manuscript. A.A. prepared the original draft. A.A. and M.D. reviewed and edited the manuscript.

Competing interests: The authors declare no competing interests.

Data availability: No original datasets were generated in this Review.

References

[1] Debnath, A., Mitra, S., Ghosh, S., Sen, R.: Understanding microbial biomineralization at the molecular level: recent advances. World Journal of Microbiology and Biotechnology **40**(10), 320 (2024) https://doi.org/10.1007/s11274-024-04132-6

[2] Jimenez-Martinez, J., Nguyen, J., Or, D.: Controlling pore-scale processes to tame subsurface biomineralization. Reviews in Environmental Science and Bio/Technology **21**(1), 27–52 (2022) https://doi.org/10.1007/s11157-021-09603-y

[3] Gao, X., Li, J., Hu, K., Zhao, Y., Han, Y., Liu, F., Tucker, M.E., Han, Z.: Calcification of cell membranes: From ions to minerals. Chemical Geology **617**, 121266 (2023) https://doi.org/10.1016/j.chemgeo.2022.121266 . Combines experiments and molecular simulations to investigate calcium–carbonate association and precursor structures near simplified biological interfaces.

[4] Schulz, H.N., Schulz, H.D.: Large sulfur bacteria and the formation of phosphorite. Science **307**(5708), 416–418 (2005) https://doi.org/10.1126/science.1103096

[5] Goldhammer, T., Br"uchert, V., Ferdelman, T.G., Zabel, M.: Microbial sequestration of phosphorus in anoxic upwelling sediments. Nature Geoscience **3**, 557–561 (2010) https://doi.org/10.1038/ngeo913

[6] Ludwig, R., Al-Horani, F.A., Beer, D., Jonkers, H.M.: Photosynthesis-controlled calcification in a hypersaline microbial mat. Limnology and Oceanography **50**(6), 1836–1843 (2005) https://doi.org/10.4319/lo.2005.50.6.1836

[7] Demichelis, R., Schuitemaker, A., Garcia, N.A., Koziara, K.B., De La Pierre, M., Raiteri, P., Gale, J.D.: Simulation of crystallization of biominerals. Annual Review of Materials Research **48**, 327–352 (2018) https://doi.org/10.1146/annurev-matsci-070317-124327

[8] Ebigbo, A., Phillips, A., Gerlach, R., Helmig, R., Cunningham, A.B., Class, H., Spangler, L.H.: Darcy-scale modeling of microbially induced carbonate mineral precipitation in sand columns. Water Resources Research **48**(7), 07519 (2012) https://doi.org/10.1029/2011WR011714

[9] Minto, J.M., Lunn, R.J., El Mountassir, G.: Development of a reactive transport model for field-scale simulation of microbially induced carbonate precipitation. Water Resources Research **55**(8), 7229–7245 (2019) https://doi.org/10.1029/2019WR025153

[10] Razbani, M.A., Jettestuen, E., Røyne, A.: Direct pore-scale numerical simulation of microbially induced calcium carbonate precipitation. Water Resources Research **59**(1), 2022–032988 (2023) https://doi.org/10.1029/2022WR032988

[11] Yuan, T., Cherkouk, A., Fischer, C.: Numerical modeling and simulation of microbially induced calcite precipitation on a cement surface at the pore scale. Advances in Water Resources **191**, 104761 (2024) https://doi.org/10.1016/j.advwatres.2024.104761

[12] Zhao, L., Filanoski, B., Chen, R., Erickson, D., Yeo, J.: Agent-based discrete element modeling of microbial-induced carbonate precipitation. Advanced Theory and Simulations **9**(3), 02233 (2026) https://doi.org/10.1002/adts.202502233 . Connects bacterial distribution, local biological activity, and extracellular polymers with simulated calcium carbonate clustering and morphology.

[13] Qiang, S., Liu, L., Li, S., Wang, S., Huang, X., Yang, J., Song, J., Zhang, Y., Huang, Y., Fan, Q.: Prediction of the non-reducing biomineralization of nuclide–microbial interactions by machine learning: The case of uranium and *Bacillus subtilis*. Toxics **13**(4), 305 (2025) https://doi.org/10.3390/toxics13040305

[14] Xiao, Y., Cao, B., Zhao, C., He, X., Fu, G., Zhao, H., Liu, H.: A review of biomineralization mechanisms and theories in micp and eicp. Journal of Rock Mechanics and Geotechnical Engineering (2026) https://doi.org/10.1016/j.jrmge.2026.05.006

[15] Oreskes, N., Shrader-Frechette, K., Belitz, K.: Verification, validation, and confirmation of numerical models in the earth sciences. Science **263**(5147), 641–646 (1994) https://doi.org/10.1126/science.263.5147.641

[16] Hommel, J., Lauchnor, E., Phillips, A., Gerlach, R., Cunningham, A.B., Helmig, R., Ebigbo, A., Class, H.: A revised model for microbially induced calcite precipitation: Improvements and new insights based on recent experiments. Water Resources Research **51**(5), 3695–3715 (2015) https://doi.org/10.1002/2014WR016503

[17] Nassar, M.K., Gurung, D., Bastani, M., Ginn, T.R., Shafei, B., Gomez, M.G.,

Graddy, C.M.R., Nelson, D.C., DeJong, J.T.: Large-scale experiments in microbially induced calcite precipitation (MICP): Reactive transport model development and prediction. Water Resources Research **54**(1), 480–500 (2018) https://doi.org/10.1002/2017WR021488 . Tests column-calibrated ureolysis kinetics against calcite accumulation in a meter-scale tank without additional fitting.

[18] Wang, X., Nackenhorst, U.: A coupled bio-chemo-hydraulic model to predict porosity and permeability reduction during microbially induced calcite precipitation. Advances in Water Resources **140**, 103563 (2020) https://doi.org/10.1016/j.advwatres.2020.103563

[19] Dittrich, M., Wehrli, B., Reichert, P.: Lake sediments during the transient eutrophication period: Reactive-transport model and identifiability study. Ecological Modelling **220**(20), 2751–2769 (2009) https://doi.org/10.1016/j.ecolmodel.2009.07.015

[20] Lu, Z., Zhou, A., Du, J., Bu, Y.: Mechanism of $CaCO_3$ nucleation during microbially induced carbonate precipitation reinforcement of siliceous sand considering surface chemistry and calcium concentration. Langmuir **41**(42), 28500–28512 (2025) https://doi.org/10.1021/acs.langmuir.5c03662

[21] Han, Z., Chen, W., Pan, D., Wang, Q., Zhao, Y., Gao, X., Zhao, Y., Han, C., Zhou, G., Liu, F., Cao, B., Li, Y., Zhu, X., Dong, H.: Experiments and simulation calculations reveal the formation pathway of struvite at the molecular level. Journal of Crystal Growth **690**, 128668 (2026) https://doi.org/10.1016/j.jcrysgro.2026.128668

[22] Wang, Z., Yang, Y., Jiang, Q., Hu, D., Li, J., Su, Y., Wang, J., Li, Y., Xing, W., Wang, S., Wang, J., Zheng, B.: The effect of crystal seeds on calcium carbonate ion pair formation in aqueous solution: A ReaxFF molecular dynamics study. Crystals **12**(11), 1547 (2022) https://doi.org/10.3390/cryst12111547

[23] Chen, Q., Wei, B., Hou, J., Liu, Y., Zhao, E., Zhou, K., Duan, L., Xie, M., Jin, Z.: Study of the influence of Na^+ and Mg^{2+} on $CaCO_3$ cluster nucleation and growth based on ReaxFF molecular dynamics simulations. The Journal of Physical Chemistry Letters **17**(1), 105–111 (2026) https://doi.org/10.1021/acs.jpclett.5c03276

[24] Demichelis, R., Raiteri, P., Gale, J.D., Quigley, D., Gebauer, D.: Stable prenucleation mineral clusters are liquid-like ionic polymers. Nature Communications **2**, 590 (2011) https://doi.org/10.1038/ncomms1604

[25] Yuan, K., Rampal, N., Du, X., Shu, F., Wang, Y., Wang, H., Stack, A.G., Ben Ishai, P., Anovitz, L.M., Xu, P.: Impact of magnetic and electric fields on the free energy to form a calcium carbonate ion-pair. Physical Chemistry Chemical Physics **26**(44), 27891–27901 (2024) https://doi.org/10.1039/D4CP02041C

[26] Di Tommaso, D., Leeuw, N.H.: The onset of calcium carbonate nucleation: A density functional theory molecular dynamics and hybrid microsolvation/continuum study. The Journal of Physical Chemistry B **112**(23), 6965–6975 (2008) https://doi.org/10.1021/jp801070b

[27] Gao, X., Han, Z., Zhao, Y., Zhang, J., Zhai, D., Li, J., Qin, Y., Liu, F., Wang, Q., Steiner, M., Han, C.: Microbial-mineral interaction experiments and density functional theory calculations revealing accelerating effects for the dolomitization of calcite surfaces by organic components. Science of the Total Environment **915**, 169971 (2024) https://doi.org/10.1016/j.scitotenv.2024.169971

[28] Piaggi, P.M., Gale, J.D., Raiteri, P.: Ab initio machine-learning simulation of calcium carbonate from aqueous solutions to the solid state. Proceedings of the National Academy of Sciences of the United States of America **122**(41), 2415663122 (2025) https://doi.org/10.1073/pnas.2415663122

[29] Wang, J., Wang, X., Xu, D.: Machine learning insights into calcium phosphate nucleation and aggregation. Acta Biomaterialia **195**, 547–558 (2025) https://doi.org/10.1016/j.actbio.2025.02.036

[30] Aykol, M., Merchant, A., Batzner, S., Wei, J.N., Cubuk, E.D.: Predicting emergence of crystals from amorphous precursors with deep learning potentials. Nature Computational Science **5**, 105–111 (2025) https://doi.org/10.1038/s43588-024-00752-y

[31] Parkhurst, D.L., Appelo, C.A.J.: Description of input and examples for PHREEQC version 3: A computer program for speciation, batch-reaction, one-dimensional transport, and inverse geochemical calculations. Techniques and Methods 6-A43, U.S. Geological Survey (2013). https://doi.org/10.3133/tm6A43

[32] Leng, Y., Soares, A.: Understanding the mechanisms of biological struvite biomineralisation. Chemosphere **281**, 130986 (2021) https://doi.org/10.1016/j.chemosphere.2021.130986

[33] McDonogh, D.P., Gale, J.D., Raiteri, P., Gebauer, D.: Redefined ion association constants have consequences for calcium phosphate nucleation and biomineralization. Nature Communications **15**, 3359 (2024) https://doi.org/10.1038/s41467-024-47721-7 . Shows how revised calcium–phosphate association constants alter predicted aqueous speciation, highlighting the importance of thermodynamic parameters.

[34] Natividad-Marin, L., Burns, M.W., Schneider, P.: A comparison of struvite precipitation thermodynamics and kinetics modelling techniques. Water Science & Technology **87**(6), 1393–1422 (2023) https://doi.org/10.2166/wst.2023.061

[35] Ribeiro, B.G.O., Gomez, M.G.: Dissolution behavior of ureolytic biocementation: Physical experiments and reactive transport modeling. Journal of Geotechnical

and Geoenvironmental Engineering **149**(9), 04023071 (2023) https://doi.org/10.1061/JGGEFK.GTENG-11275

[36] Borrok, D., Turner, B.F., Fein, J.B.: A universal surface complexation framework for modeling proton binding onto bacterial surfaces in geologic settings. American Journal of Science **305**(6–8), 826–853 (2005) https://doi.org/10.2475/ajs.305.6-8.826

[37] Fein, J.B.: Thermodynamic modeling of metal adsorption onto bacterial cell walls: Current challenges. In: Sparks, D.L. (ed.) Advances in Agronomy vol. 90, pp. 179–202. Elsevier, Amsterdam (2006). https://doi.org/10.1016/S0065-2113(06)90005-4

[38] Thomas, K.J., Rice, C.V.: Revised model of calcium and magnesium binding to the bacterial cell wall. BioMetals **27**(6), 1361–1370 (2014) https://doi.org/10.1007/s10534-014-9797-5

[39] Fein, J.B.: Advanced biotic ligand models: Using surface complexation modeling to quantify metal bioavailability to bacteria in geologic systems. Chemical Geology **464**, 127–136 (2017) https://doi.org/10.1016/j.chemgeo.2016.10.001

[40] Nishimura, I., Matsubara, H.: Coupling simulation of microbially induced carbonate precipitation and bacterial growth using reaction–diffusion and homogenisation systems. Acta Geotechnica **16**(5), 1315–1330 (2021) https://doi.org/10.1007/s11440-021-01178-w

[41] Nishimura, I., Matsubara, H.: Electricity-reaction–diffusion system for microbially induced carbonate precipitation. Soils and Foundations **62**(5), 101217 (2022) https://doi.org/10.1016/j.sandf.2022.101217

[42] Nishimura, I., Matsubara, H.: Numerical modelling of biomineralization by photoautotrophic microorganisms on the outcrop. International Journal of Rock Mechanics and Mining Sciences **202**, 106518 (2026) https://doi.org/10.1016/j.ijrmms.2026.106518

[43] Faeli, Z., Montoya, B.M., Gabr, M.A.: Elucidating factors governing MICP biogeochemical processes at macro-scale: A reactive transport model development. Computers and Geotechnics **160**, 105514 (2023) https://doi.org/10.1016/j.compgeo.2023.105514

[44] Wang, Y.-j., Chen, W.-b., Li, P.-l., Yin, Z.-y., Yin, J.-h., Jiang, N.-j.: Soil improvement using biostimulated MICP: Mechanical and biochemical experiments, reactive transport modelling, and parametric analysis. Computers and Geotechnics **172**, 106446 (2024) https://doi.org/10.1016/j.compgeo.2024.106446

[45] Li, X., Tao, J., Paassen, L.A.: Reactive transport modeling of microbial-induced

calcite precipitation treatment through shallow underwater injection. Computers and Geotechnics **174**, 106601 (2024) https://doi.org/10.1016/j.compgeo.2024.106601

[46] Qin, C.-Z., Hassanizadeh, S.M., Ebigbo, A.: Pore-scale network modeling of microbially induced calcium carbonate precipitation: Insight into scale dependence of biogeochemical reaction rates. Water Resources Research **52**(11), 8794–8810 (2016) https://doi.org/10.1002/2016WR019128 . Uses pore-network modeling to investigate how mass transfer and spatial scale influence MICP reaction rates, providing a computational assessment of scale dependence.

[47] Feng, D., Chu, Y., Feng, L., Wang, L., Huang, Y.: Pore-scale modeling of the MICP process by using a coupled FEM-LBM-CA model: With a focus on the heterogeneity of the pore structures. Computers and Geotechnics **172**, 106414 (2024) https://doi.org/10.1016/j.compgeo.2024.106414

[48] Yang, E., Baek, S., Kwon, T.H., Yun, T.S.: X-ray ct-based interpretation of microbial-induced carbonate precipitation and local hydraulic behaviors. Engineering Geology **330**, 107426 (2024) https://doi.org/10.1016/j.enggeo.2024.107426

[49] Zhang, T., Klapper, I.: Critical occlusion via biofilm induced calcite precipitation in porous media. New Journal of Physics **16**(5), 055009 (2014) https://doi.org/10.1088/1367-2630/16/5/055009

[50] Starnoni, M., Sanchez-Vila, X.: Pore-scale modelling of subsurface biomineralization for carbon mineral storage. Advances in Water Resources **185**, 104641 (2024) https://doi.org/10.1016/j.advwatres.2024.104641

[51] Dawi, M.A., Starnoni, M., Porta, G., Sanchez-Vila, X.: Pore-scale coupling of flow, biofilm growth, and nutrient transport: A microcontinuum approach. Water Resources Research **60**(11), 2024–038393 (2024) https://doi.org/10.1029/2024WR038393

[52] Li, B., Taniguchi, D., Gedara, J.P., Gogulancea, V., Gonzalez-Cabaleiro, R., Chen, J., McGough, A.S., Ofiteru, I.D., Curtis, T.P., Zuliani, P.: NUFEB: A massively parallel simulator for individual-based modelling of microbial communities. PLOS Computational Biology **15**(12), 1007125 (2019) https://doi.org/10.1371/journal.pcbi.1007125

[53] Zi, J., Liu, T., Zhang, W., Pan, X., Ji, H., Zhu, H.: Quantitatively characterizing sandy soil structure altered by MICP using multi-level thresholding segmentation algorithm. Journal of Rock Mechanics and Geotechnical Engineering **16**(10), 4285–4299 (2024) https://doi.org/10.1016/j.jrmge.2023.11.025

[54] Filanoski, B.E., Bobal, M.L., Phinney, K.R., Hull, D.R., Erickson, D.: Biocementation shows a three-dimensional geometry dependence in microfluidic

pore networks mapped by deep-learning segmentation. Lab on a Chip **26**(18), 4903–4912 (2026) https://doi.org/10.1039/D6LC00125D

[55] Li, Y., Prabhu, A., Hou, B., Wong, M.L., Lu, A., Xing, J., Ngo, D., Xu, B., Hazen, R.M.: Mineral biosignature identification from raman spectroscopy using machine learning. PNAS Nexus **5**(7), 215 (2026) https://doi.org/10.1093/pnasnexus/pgag215 . Uses interpretable analysis of Raman spectra to distinguish biotic and abiotic apatite, illustrating mineral classification rather than forecasting mineral formation

[56] Wang, Y., Zheng, C., Su, R., Fan, L., Chang, M., Liu, N., Li, F., Wu, J.: Coupling bayesian optimization and multi-paradigm ensemble learning to predict lead remediation in microbially induced carbonate precipitation: From model performance to crystalline control windows. Journal of Hazardous Materials **508**, 141918 (2026) https://doi.org/10.1016/j.jhazmat.2026.141918

[57] Talamkhani, S.: Machine learning-based prediction of unconfined compressive strength of sands treated by microbially-induced calcite precipitation (MICP): A gradient boosting approach and correlation analysis. Advances in Civil Engineering **2023**, 3692090 (2023) https://doi.org/10.1155/2023/3692090

[58] El-Sekelly, W., Raja, M.N.A., Abdoun, T.: Explainable AI for predicting the strength of bio-cemented sands. Journal of Rock Mechanics and Geotechnical Engineering **18**(2), 1552–1569 (2026) https://doi.org/10.1016/j.jrmge.2025.05.029

[59] Fu, Y., Tong, H., Yuan, J., Cui, J., Shan, Y.: Prediction of interparticle parameters of MICP-treated calcareous sand based on the CNN-BiLSTM-Attention and XGBoost hybrid models. Journal of Rock Mechanics and Geotechnical Engineering (2025) https://doi.org/10.1016/j.jrmge.2025.10.001

[60] Scheurer, S., Reiser, P., Brünnette, T., Nowak, W., Guthke, A., Bürkner, P.-C.: Uncertainty-aware surrogate-based amortized bayesian inference for computationally expensive models. Transactions on Machine Learning Research (2026). Accounts for surrogate-model uncertainty during parameter inference for MICP reactive-transport simulations, reducing overconfidence in inferred quantities.

[61] Verlet, L.: Computer "experiments" on classical fluids. i. thermodynamical properties of lennard-jones molecules. Physical Review **159**(1), 98–103 (1967) https://doi.org/10.1103/PhysRev.159.98

[62] Raiteri, P., Demichelis, R., Gale, J.D.: Development of accurate force fields for the simulation of biomineralization. In: Methods in Enzymology vol. 532, pp. 3–23 (2013). https://doi.org/10.1016/B978-0-12-416617-2.00001-1

[63] Li, Y., Zeng, H., Zhang, H.: Atomistic simulations of nucleation and growth of $CaCO_3$ with the influence of inhibitors: A review. Materials Genome Engineering

Advances **1**(1), 4 (2023) https://doi.org/10.1002/mgea.4

[64] Huang, M., Zheng, X., He, X., Lin, X., Ye, J.: *Paenibacillus mucilaginosus*-induced CO_2 fixation into amorphous and crystalline carbonate minerals. Process Biochemistry **157**, 242–255 (2025) https://doi.org/10.1016/j.procbio.2025.07.017

[65] Wang, P., Yang, X.: Elucidating deposition process of calcium carbonate and mechanical properties of precipitation via molecular dynamics simulation. Surfaces and Interfaces **49**, 104460 (2024) https://doi.org/10.1016/j.surfin.2024.104460

[66] Senftle, T.P., Hong, S., Islam, M.M., Kylasa, S.B., Zheng, Y., Shin, Y.K., Junkermeier, C., Engel-Herbert, R., Janik, M.J., Aktulga, H.M., Verstraelen, T., Grama, A., Duin, A.C.T.: The ReaxFF reactive force-field: development, applications and future directions. npj Computational Materials **2**, 15011 (2016) https://doi.org/10.1038/npjcompumats.2015.11

[67] Qin, L., Mao, X., Cui, Y., Bao, J., Sant, G., Chen, T., Zhang, P., Gao, X., Bauchy, M.: New insights into the early stage nucleation of calcium carbonate gels by reactive molecular dynamics simulations. The Journal of Chemical Physics **157**(23), 234501 (2022) https://doi.org/10.1063/5.0127240

[68] Torrie, G.M., Valleau, J.P.: Nonphysical sampling distributions in monte carlo free-energy estimation: Umbrella sampling. Journal of Computational Physics **23**(2), 187–199 (1977) https://doi.org/10.1016/0021-9991(77)90121-8

[69] Laio, A., Parrinello, M.: Escaping free-energy minima. Proceedings of the National Academy of Sciences of the United States of America **99**(20), 12562–12566 (2002) https://doi.org/10.1073/pnas.202427399

[70] Barducci, A., Bonomi, M., Parrinello, M.: Metadynamics. Wiley Interdisciplinary Reviews: Computational Molecular Science **1**(5), 826–843 (2011) https://doi.org/10.1002/wcms.31

[71] Fang, M., Qin, L., Guo, T., Zang, H., Tu, Y., Ji, Y.: ReaxFF metadynamics reveals the localized passivation effects of carbonate ion on tricalcium silicate surface hydration. Cement and Concrete Research **203**, 108179 (2026) https://doi.org/10.1016/j.cemconres.2026.108179

[72] Duignan, T.T.: The potential of neural network potentials. ACS Physical Chemistry Au **4**(3), 232–241 (2024) https://doi.org/10.1021/acsphyschemau.4c00004

[73] Morel, F.M.M., Hering, J.G.: Principles and Applications of Aquatic Chemistry. John Wiley & Sons, New York (1993)

[74] Stumm, W., Morgan, J.J.: Aquatic Chemistry: Chemical Equilibria and Rates in Natural Waters, 3rd edn. John Wiley & Sons, New York (1996)

[75] De Yoreo, J.J., Vekilov, P.G.: Principles of crystal nucleation and growth. Reviews in Mineralogy and Geochemistry **54**(1), 57–93 (2003) https://doi.org/10.2113/0540057

[76] Zahn, D.: Thermodynamics and kinetics of prenucleation clusters, classical and non-classical nucleation. ChemPhysChem **16**(10), 2069–2075 (2015) https://doi.org/10.1002/cphc.201500231

[77] De Yoreo, J.J., Gilbert, P.U.P.A., Sommerdijk, N.A.J.M., Penn, R.L., Whitelam, S., Joester, D., Zhang, H., Rimer, J.D., Navrotsky, A., Banfield, J.F., Wallace, A.F., Michel, F.M., Meldrum, F.C., Cölfen, H., Dove, P.M.: Crystallization by particle attachment in synthetic, biogenic, and geologic environments. Science **349**(6247), 6760 (2015) https://doi.org/10.1126/science.aaa6760

[78] Paulo, C., Kenney, J.P.L., Persson, P., Dittrich, M.: Effects of phosphorus in growth media on biomineralization and cell surface properties of marine cyanobacteria synechococcus. Geosciences **8**(12), 471 (2018) https://doi.org/10.3390/geosciences8120471

[79] Dittrich, M., Müller, B., Mavrocordatos, D., Wehrli, B.: Induced calcite precipitation by cyanobacterium Synechococcus. Acta Hydrochimica et Hydrobiologica **31**(2), 162–169 (2003) https://doi.org/10.1002/aheh.200300486

[80] Obst, M., Wehrli, B., Dittrich, M.: CaCO3 nucleation by cyanobacteria: laboratory evidence for a passive, surface-induced mechanism. Geobiology **7**(3), 324–347 (2009) https://doi.org/10.1111/j.1472-4669.2009.00200.x

[81] Qin, W., Wang, C.-y., Ma, Y.-x., Shen, M.-j., Li, J., Jiao, K., Tay, F.R., Niu, L.-n.: Microbe-mediated extracellular and intracellular mineralization: Environmental, industrial, and biotechnological applications. Advanced Materials **32**(22), 1907833 (2020) https://doi.org/10.1002/adma.201907833

[82] Ramos, O., Kwon, T.H.: Development of bio-grout injection strategy and design guide using reactive transport model for field-scale soil improvement based on microbially induced calcium carbonate precipitation (MICP). Geomechanics for Energy and the Environment **36**, 100509 (2023) https://doi.org/10.1016/j.gete.2023.100509

[83] Razbani, M.A., Røyne, A., Jettestuen, E.: A one-dimensional reactive transport model for microbially induced calcium carbonate precipitation (MICP) in PHREEQC. Geomicrobiology Journal **42**(1), 19–29 (2025) https://doi.org/10.1080/01490451.2024.2425295

[84] Kumar, D., Sharma, A.K.: Spatio-temporal reactive transport modeling of microbially induced calcite precipitation and porosity evolution in porous media. Geomicrobiology Journal **43**(7), 850–871 (2026) https://doi.org/10.1080/01490451.2026.2667827

[85] Ma, G., Xiao, Y., Zhang, J., Zhang, Z.: Relating solution tests to pore-scale $caco_3$ crystal growth: Numerical simulation based on the phase field method. Computers and Geotechnics **193**, 107947 (2026) https://doi.org/10.1016/j.compgeo.2026.107947

[86] Li, X., Yang, X.: porousrtfoam v1.0: An open-source numerical platform for simulating pore-scale reactive transport processes in porous media. Environmental Modelling & Software **187**, 106396 (2025) https://doi.org/10.1016/j.envsoft.2025.106396

[87] Murugan, R., Sundararaghavan, A., Dhami, N.K., Mukherjee, A., Suraishkumar, G.K.: Importance of carbon to nitrogen ratio in microbial cement production: Insights through experiments and genome-scale metabolic modelling. Biochemical Engineering Journal **186**, 108573 (2022) https://doi.org/10.1016/j.bej.2022.108573

[88] Raissi, M., Perdikaris, P., Karniadakis, G.E.: Physics-informed neural networks: A deep learning framework for solving forward and inverse problems involving nonlinear partial differential equations. Journal of Computational Physics **378**, 686–707 (2019) https://doi.org/10.1016/j.jcp.2018.10.045

[89] Arab, A., Scheytt, T., Nagel, T., Taherdangkoo, R.: Physics-informed neural network surrogate for reactive nitrate transport in groundwater. Advances in Water Resources **213**, 105305 (2026) https://doi.org/10.1016/j.advwatres.2026.105305

[90] Zeng, C., Veenis, Y., Hall, C.A., Young, E.S., Star, W.R.L., Zheng, J.-j., Paassen, L.A.: Experimental and numerical analysis of a field trial application of microbially induced calcite precipitation for ground stabilization. Journal of Geotechnical and Geoenvironmental Engineering **147**(7), 05021003 (2021) https://doi.org/10.1061/(ASCE)GT.1943-5606.0002545